The paralogous ArsR1 and ArsR2 regulators of *Pseudomonas putida* KT2440 as basis for arsenic biosensor development

Matilde Fernández[1], Bertrand Morel[1]*, Juan L. Ramos[1,2] and Tino Krell[1]#

[1] Department of Environmental Protection, Estación Experimental del Zaidín, Consejo Superior de Investigaciones Científicas, C/ Prof. Albareda, 1, 18008 Granada, Spain

[2] Biotechnology Technological Area, Abengoa Research, Calle Energía Solar 1, Building E, Campus Palmas Altas, 41014, Sevilla, Spain

Address correspondence to Tino Krell, e-mail: tino.krell@eez.csic.es

*Present address: Departamento de Química Física, Facultad de Ciencias, Universidad de Granada, 18071 Granada, Spain

M.F. and B.M. contributed equally to this work

Running title: ArsR paralogues of *Pseudomonas putida*

Abstract

The remarkable metal resistance of many microorganisms is related to the presence of multiple metal resistance operons. *Pseudomonas putida* KT2440 can be considered as a model for these microorganisms since its arsenic resistance is due to the action of proteins encoded by the two paralogous arsenic resistance operons *ars1* and *ars2*. Both operons contain the genes encoding for transcriptional regulators ArsR1 and ArsR2 that control operon expression. We show here that purified ArsR1 and ArsR2 bind the trivalent salt of arsenic (arsenite) with similar affinity of 30 μM, whereas no binding is observed for the pentavalent salt (arsenate). Furthermore, trivalent salts of bismuth and antimony showed binding to both paralogues. The position of cysteines, found to bind arsenic in other homologues, indicates that ArsR1 and ArsR2 employ different modes for arsenite recognition. Both paralogues are dimeric and possess significant thermal stability. Both proteins were used to construct whole-cell, *lacZ*-based biosensors. Whereas responses to bismuth were negligible, significant responses were observed for arsenite, arsenate and antimony. Biosensors based on the *P. putida arsB1/arsB2* arsenic efflux pump double mutant were significantly more sensitive than biosensors based on the wild-type strain. This sensitivity enhancement by pump mutation may be a convenient strategy for the construction of other biosensors. A frequent limitation found for other arsenic biosensors was their elevated background signal and interference by inorganic phosphate. Biosensors constructed show no interference by inorganic phosphate, are characterized by a very low background signal and were found suitable to analyze environmental samples.

Importance

Arsenic is top on the priority list of hazardous compounds issued by the US Agency for Toxic Substances and Disease. The reason for the stunning arsenic resistance of many microorganisms is the existence of paralogous arsenic resistance operons. *Pseudomonas putida* KT2440 is a model organism for such bacteria and their duplicated *ars* operons and in particular their ArsR transcription regulators have been studied in depth by *in vivo* approaches. Here we present an analysis of both purified ArsR paralogues by different biophysical techniques, and data obtained provide valuable insight into their structure and function. Particularly insightful was the comparison of ArsR effector profiles determined by *in vitro* and *in vivo* experimentation. We also report the use of both paralogues to construct robust and highly sensitive arsenic biosensors. Our finding that the deletion of both arsenic efflux pumps significantly increases biosensor sensitivity, is of general relevance in the biosensor field.

Introduction

Arsenic is omnipresent in nature and found in many environmental biotopes like sea and fresh water, soils or rocks. It is either released through various natural processes such as weathering or hydrothermal emissions or generated by a number of anthropogenic activities like the use of arsenic containing pesticides, mining activities or combustion of fossil fuels (1, 2).

Arsenic is very toxic and was found to be associated with an increased risk of a wide range of health issues including cancers of the skin, lung, bladder, liver, and kidney as well as neurological and cardiovascular disease (3). The toxicity of arsenic, combined with its omnipresence in nature represents a world-wide health concern (4). In fact, it was placed first on the priority list of hazardous compounds issued by The United States Agency for Toxic Substances and Disease Registry (http://www.atsdr.cdc.gov/SPL/index.html). Of particular relevance is the groundwater contamination with arsenic in Asiatic countries (5, 6) and environmental arsenic monitoring is thus of primary importance (7, 8).

At neutral pH, arsenic is mostly found as trivalent arsenite or pentavalent arsenate. The principles of toxicity differ for both forms. Whereas arsenite toxicity can be associated with its ability to react with sulfhydryl groups in proteins, the harmful effects caused by arsenate are associated with its capacity to mimic phosphate groups in a wide number of cellular reactions (9, 10). Bacteria have developed many strategies in response to the environmental presence of arsenic (1). One of these strategies consists of the extrusion of arsenic and the corresponding proteins are encoded by *ars* operons. The minimal set of *ars* operon genes, consisting of the *arsR* regulator (11), the transmembrane *arsB* arsenite efflux pump and the arsenate reductase *arsC,* has been observed in a number of different bacteria (12). Interestingly, several strains like

78 *Pseudomonas putida* KT2440 (13-15), *Corynebacterium glutamicum* (16) or
79 *Ochrobactrum tritici* (17) possess two functional copies of the *ars* operon providing
80 high arsenic resistance.

81 The present study was conducted using *P. putida* KT2440, which is a
82 metabolically versatile soil bacterium that serves as a model not only to study metal
83 resistance but also in the fields of bioremediation, plant–microbe interactions or
84 bacterial signaling (18-20). Strain KT2440 is highly resistant to arsenic but also to other
85 metaloids and heavy metals and genome analyses indicated that several resistance
86 systems are duplicated (21). The two *ars* operon copies of *P. putida* KT2440, termed
87 *ars1* and *ars2*, show a high degree of sequence identity and are extended by the *arsH*
88 gene encoding an organoarsenical oxidase (22) (Fig. 1). Different aspects of the two *ars*
89 operons in *P. putida* KT2440 have been recently reported. The *ars2* operon was found
90 to be present in the core genome of *P. putida* strains whereas the existence of *ars1* is
91 specific to KT2440 and may have been acquired by horizontal gene transfer (14). The
92 gene products of both operons work synergistically which may account for the high
93 arsenite tolerance of the strain (14). Another study reported that the effects of *ars1* and
94 *ars2* are not additive at the optimal growth temperature of 30 ºC, whereas at 15 ºC the
95 contribution of *ars2* to arsenite resistance was largely superior to that mediated by the
96 *ars1* system (15).

97 ArsR together with the SmtB regulator gives a name to a family of regulators
98 that can be associated with heavy metal resistance (23). Members of the ArsR/SmtB
99 protein family operate by a de-repression mechanism, where apo-repressors are DNA
100 bound and the binding of different heavy metals causes protein dissociation and
101 transcriptional activation. The ArsR protein of *E. coli* has been shown *in vitro* to bind
102 arsenite as well as the trivalent salts of bismuth and antimony (24, 25). *In vivo* studies

show that arsenate, in addition to these three compounds, cause transcriptional activation (24). The *in vivo* effect of arsenate is caused by its cellular conversion into arsenite by the arsenate reductase ArsC (24). Members of the ArsR family share the same overall structure (26). Arsenite binds to ArsR proteins via three cysteine residues. However, experiments conducted with regulators from *E. coli* (27), *Corynebacterium glutamicum* (28) and *Acidithiobacillus ferrooxidans* (29) has resulted in the identification of three different arsenite binding modes, characterized by distinct cysteine binding motifs that are located in different parts of the structures (Supp. Fig. 1). The ArsR1 and ArsR2 paralogues of *P. putida* KT2440 share 56 % of sequence identity amongst each other (Supp. Fig. 1). As indicated in Supp. Fig. 1 the position of cysteine residues differs in ArsR1 and ArsR2 and is, in addition, different to the ArsR proteins studied from *E. coli, C. glutamicum* or *A. ferrooxidans*. This indicates that arsenite recognition at ArsR1 and ArsR2 occurs yet by another cysteine motif (Supp. Fig. 1). It has been proposed that the evolution of spatially unrelated arsenite binding sites is the result of convergent evolution (28).

The two ArsR paralogues of *P. putida* KT2440 is a model system to understand the concerted action of paralogous regulators on metal resistance (14, 15). We report here the generation of purified, recombinantly produced ArsR1 and ArsR2 and its analysis by an array of biochemical and biophysical approaches. As mentioned above environmental arsenic monitoring is of central importance and several ArsR-based biosensors have been described (30, 31). In the second part of this work we describe the construction of ArsR1 and ArsR2 based biosensors. We demonstrate that biosensors based on a mutant of both arsenite efflux pumps, ArsB1 and ArsB2, possess a higher sensitivity as compared to wild-type (wt) based sensors. The finding that efflux pump

Applied and Environmental Microbiology

mutation translates into a significant increase in sensitivity of the corresponding sensor is of general relevance for biosensor construction.

Applied and Environmental Microbiology

130 **Materials and Methods**

131 *Materials:* $NaAsO_2$, Na_2HAsO_4, $SbCl_3$, $Bi(NO_3)_3$ and NaH_2PO_4 (referred throughout this
132 article as arsenite, arsenate, antimony, bismuth or inorganic phosphate, respectively)
133 were purchased from Sigma-Aldrich.
134
135 *Strains and culture conditions:* Strains and plasmids used in this study are listed in
136 Table 1. *P. putida* KT2440 and its isogenic double mutant in *arsB1*/*arsB2* (14) were
137 grown in M9 with 5 mM glucose as a carbon source or LB medium at 30 °C with
138 shaking, unless otherwise stated. *Escherichia coli* DH5α, the host for gene cloning, was
139 cultured in LB medium at 37ºC. When required, antibiotics were added to the following
140 final concentrations: chloramphenicol (Cm), 30 µg/ml; kanamycin (Km), 25 µg/ml;
141 gentamycin (Gm), 30 µg/ml; tetracycline (Tc), 10 µg/ml.
142
143 *Construction of expression plasmids for ArsR1 and ArsR2, cell culture and protein*
144 *purification:* The *arsR1* and *arsR2* sequences were amplified by PCR using specific
145 primers containing NdeI and XhoI restriction sites (Table 2). The PCR products were
146 digested with the corresponding enzymes and cloned into pET28a (Novagen) previously
147 cleaved with the same enzymes. Ligation mixtures were used to electroporate *E. coli*
148 DH5α and colonies were selected on LB plates containing Km. Resulting plasmids
149 (pET_arsR1 and pET_arsR2) were verified by sequencing the insert and flanking
150 regions. *E. coli* BL21 (DE3) was transformed with either pET_arsR1 or pET_arsR2.
151 Cultures were grown in 2 l Erlenmeyer flasks containing 400 ml LB supplemented with
152 25 µg ml^{-1} kanamycin, at 37 ºC until the culture reached an OD_{660} of 0.6. At this point
153 protein expression was induced by the addition of 0.1 mM isopropyl β-D-1-
154 thiogalactopyranoside. Growth was continued at 18 ºC overnight prior to cell harvest by

centrifugation (15 min, 4 400 x g). All manipulations were carried out at 4 ºC. The pellet was resuspended in buffer A (20 mM Tris/HCl, 500 mM NaCl, 10 mM imidazole, 10 % (v/v) glycerol, 10 mM β-mercaptoethanol, pH 8.5), sonicated for cell rupture and centrifuged at 20 000 x g for 1 hour. The supernatant was filtered and loaded onto a 5 ml HisTrap HP column (Amersham GE Healthcare) previously equilibrated with buffer A. Proteins were eluted using an imidazole gradient (0 - 1 M) in buffer A. Protein purity was assessed by SDS-PAGE and pooled fractions were dialyzed into analysis buffer (20 mM Hepes, 150 mM NaCl, 2 mM tris(2-carboxyethyl)phosphine) (TCEP), pH 7.2) unless otherwise stated. Sample concentrations were determined by Bradford assay and by measurement of the absorbance at 280 nm using the theoretical extinction coefficient of 19730 M^{-1} cm^{-1} determined for both proteins as by the Expasy ProtParam algorithm (32).

Analytical size exclusion chromatography: Analytical size exclusion chromatography experiments were conducted using an Åkta FLPC system (Amersham GE Healthcare). Purified protein (at 25 µM) was loaded onto a Superdex-200 10/300GL column (Amersham GE Healthcare) previously equilibrated in analysis buffer. The elution was performed at a constant flow rate of 0.4 ml/min and the absorbance of the eluate was monitored at 280 nm. The molecular mass of the ArsR paralogues was estimated from a calibration curve constructed from the analysis of the following standards: cytochrome c (12.4 kDa), carbonic anhydrase (29 kDa), bovine serum albumin (monomer, 66 kDa, and dimer, 132 kDa) and β-amylase (200 kDa).

Circular Dichroism (CD) spectroscopy: CD measurements were performed with a Jasco J-715 spectropolarimeter (Tokyo, Japan) equipped with a thermostatized cell holder.

Applied and Environmental Microbiology

Measurements of the far-UV CD spectra (260-200 nm) were made with a 1 mm path length quartz cuvette at a protein concentration of 10 µM in analysis buffer. Spectra were recorded at a scan rate of 100 nm/min, 1 nm step resolution, 1 s response and 1 nm bandwidth. Spectra shown are averages of 5 scans. Spectra were corrected by baseline subtraction using the buffer spectrum and the CD signal was normalized to mean residue molar ellipticity ([θ], in $deg.dmol^{-1}cm^{2}$). The spectra were deconvoluted to determine the relative abundance of secondary structure elements using the CDNN software package (33).

Differential scanning calorimetry (DSC): DSC experiments were carried out on a VP capillary cell microcalorimeter (MicroCal Northampton, MA). The temperature range from 5ºC to 85ºC was scanned at a rate of 180°C/h. The calorimetric cells (operating volume 0.134 ml) were kept under an excess pressure of 60 psi bar to prevent degassing. Several buffer-buffer baselines were obtained before each protein run to ascertain proper instrument equilibration. Protein samples were exhaustively dialyzed at 4ºC against analysis buffer. The protein concentration was 20 µM and arsenite and arsenate were added at a concentration of 250 µM. Thermograms were normalized using the concentration of protein monomers.

Intrinsic tryptophan fluorescence spectroscopy: Measurements were made on a PTI QM-2003 fluorimeter with a Xenon lamp as a light source (Photon Technology International, Lawrenceville, NJ) at 25ºC using an excitation wavelength of 290 nm and slit widths of 5 nm. Tryptophan emission spectra were recorded from 300 to 400 nm. Spectra were taken in 1 nm increments with 1 s of integration per increment. Protein samples of 5 µM were prepared in analysis buffer. Titrations were conducted with

freshly prepared solutions of arsenite (1 mM stock solution), antimony and bismuth. Due to the low solubility of antimony and bismuth, these stock solutions were prepared in methanol at a concentration of 20 mM and 2 mM, respectively. Quenching of tryptophan emission was performed by successive additions of the ligands to the cuvette, followed by gentle sample mixing, incubation for 2 min and spectra recording. The fluorescence intensities were corrected for absorption of the exciting light and reabsorption of the emitted light to decrease the inner filter effect using the equation:

$$F_{corr} = F_{obs} * 10^{(Aexc+Aem)/2}$$

where F_{corr} is the corrected fluorescence value, F_{obs} the measured fluorescence value, A_{exc} the absorption value at the excitation wavelength, and A_{em} the absorption value at the emission wavelength (34). Spectra were then normalized by the total protein concentration after each titration and the starting fluorescence signal was set to 100 % fluorescence. Fluorescence titration curves were fitted in Origin using the equation for one binding site to determine the dissociation constants.

Electrophoretic mobility shift assays (EMSA): DNA fragments of approximately 500 bp containing the P_{ars1} and P_{ars2} promoter regions were amplified by PCR using the primer pairs Pars1_for/Pars1_rev and Pars2_for/Pars2_rev, respectively (Table 2). Amplified DNA was isolated from agarose gels and end-labeled with [γ-^{32}P] deoxy-ATP using T4 polynucleotide kinase. A 10 µl sample containing 2 nM labeled DNA (1.5 x 10^4 cpm) was incubated at 30ºC with various concentrations of purified ArsR for 15 min in binding buffer (10 mM Tris/HCl, 20 mM NaCl, 100 mM Mg acetate, 0.02 mM EDTA, 0.2 mM DTT, 1 % (v/v) glycerol, pH 7.5) containing 20 µg/ml of poly(dI-dC) and 200

µg/ml bovine serum albumin. The DNA protein complexes were resolved by electrophoresis in 4 % (w/v) non-denaturing polyacrylamide gels at 50 volts for 3 hours in 50 mM Tris/HCl, 20 mM glycine, pH 7.8. The gels were dried and analyzed with a GS525 molecular imager (Bio- Rad).

*Construction of arsenic biosensors***:** The *ars1* and *ars2* genes besides their respective promoter regions were amplified by PCR using primers ars1biosen_for (EcoRI) and ars1biosen_rev (PstI) (for *ars1*) and ars2biosen_for (EcoRI) and ars2biosen_rev (XbaI) (for *ars2*). The Expand High Fidelity PCR System (Roche) was used on all PCR amplifications. PCR products were cleaned using a QIAquick PCR Purification Kit (Qiagen) and then cloned into pMP220 digested with the corresponding enzymes. Ligation mixtures were electroporated into *E. coli* and clones were selected on Tc containing LB plates. Clones were verified by plasmid restriction analysis and DNA-sequencing. The resulting plasmids, pBiosen_arsR1 and pBiosen_arsR2, were transferred into *P. putida* KT2240 and its *arsB1*/*arsB2* double mutant.

β-galactosidase assays: Overnight cultures were diluted 50-fold in LB medium supplemented with different ArsR ligand concentrations and incubated with shaking until an OD_{600} of 0.8. Assays were carried out on permeabilized cells as previously described (35). Data shown are means and standard deviations from three independent experiments each conducted in duplicate.

Inductively coupled plasma-optical emission spectroscopy (ICP-OES): These analyses were carried out by the scientific instrumentation service of the Estación Experimental del Zaidín (Granada, Spain, http://www.eez.csic.es/?q=es/node/1187).

Results

Generation of recombinant ArsR1 and ArsR2

ArsR1 and ArsR2 of *P. putida* KT2440 were overexpressed in *E. coli* and purified from the soluble fraction of the cell lysate by affinity chromatography. Relatively modest average yields of 2 and 4 mg of pure protein per liter of *E. coli* culture were obtained for ArsR1 and ArsR2, respectively. Far-UV circular dichroism (CD) experiments of ArsR1 and ArsR2 were carried out to assess their secondary structure (Fig. 2A). The spectra of both proteins were very similar indicating that ArsR1 and ArsR2 possess similar secondary structure content. The curves showed minima at 208 nm and around 220-222 nm characteristic of α-helical elements. The deconvolution of spectra resulted in 42 and 41 % of α-helix for ArsR1 and ArsR2, respectively; as well as 28 and 29 % random coil for both proteins. Attempts to make homology models were only successful in the case of ArsR1 (Supp. Fig. 2), but the high degree of sequence similarity suggests that both proteins share a similar secondary structure content. This model shows 41 % α-helix assuming a non-helical conformation of the His-tag (not modelled). The agreement of the experimentally determined α-helical contents with that derived from the homology model, strongly suggests that proteins purified are in their folded and active state.

ArsR1 and ArsR2 are dimeric in solution

To determine the oligomeric state of both proteins, analytical size exclusion chromatography experiments were carried out showing that both proteins eluted as a single symmetric peak (Fig. 3). Eluted proteins were submitted to SDS-PAGE which resulted in the confirmation of the molecular integrity of both proteins (Supp. Fig. 3). With the help of standard curves (Fig. 3) apparent molecular mass of 28 kDa and 26

kDa were determined for ArsR1 and ArsR2, respectively. Considering the sequence derived mass of ArsR1 and ArsR2 monomers (15 757 Da and 15 407 Da respectively), we conclude that both proteins are dimeric in solution. To assess the effect of arsenite and arsenate on the oligomeric state of both proteins, experiments were repeated in the presence of 1 mM arsenite or arsenate, which was added to the protein sample and the gel filtration buffer. The obtained chromatograms are highly similar to those recorded in the absence of ligand (Fig. 3), indicating that ligand binding does not alter the protein oligomeric state.

The ArsR paralogues unfold in a single event at temperatures beyond 60 ºC

Protein stability of both paralogues was analyzed by Differential Scanning Calorimetry (DSC). This technique permits the determination of the Tm value, which corresponds to the temperature at which half the protein is unfolded and the remaining part in its native state, as well as the enthalpy change upon unfolding. The DSC thermograms of both proteins (Fig. 2B) show that both proteins possess significant thermal stabilities and Tm values of 61.5 and 71.1 ºC were determined for ArsR1 and ArsR2, respectively (Table 3). At the end of the temperature up-scan, samples were cooled to 5ºC and no unfolding events were observed in the subsequent up-scan indicating that protein unfolding is irreversible.

ArsR paralogues bind arsenite with similar affinities

In vivo the ArsR transcriptional regulators mediate responses to arsenate and arsenite (12, 36). Since both compounds can be interconverted in the cell it is unclear whether both compounds or only one of them is recognized by the regulators. Ligand binding typically causes increases in the thermal stability of proteins and consequently

306 the Tm value (37). To study ligand binding at ArsR1 and ArsR2, DSC studies were
307 repeated in the presence of saturating concentrations of arsenate and arsenite. Due to the
308 structural similarities between inorganic phosphate and arsenite/arsenate it has been
309 observed in the past that these ligands are recognized by the same receptor protein (38-
310 40). To assess this issue, DSC analyses were also carried out in the presence of
311 inorganic phosphate. The corresponding thermograms (Fig. 4) showed an increase in
312 Tm exclusively in the presence of arsenite. Apart from the increase in Tm (Table 3)
313 protein folding occurred in two sequential events. Importantly, the Tm of the major
314 unfolding event in the presence of arsenite was approximately 12 and 16 degree higher
315 than that of the ligand free protein. In marked contrast, the thermograms (Fig. 4) and
316 derived unfolding parameters in the presence of arsenate and inorganic phosphate
317 (Table 3) are almost identical to the apo-proteins. These data show that arsenite but not
318 arsenate nor inorganic phosphate bind to ArsR1 and ArsR2.
319 To determine the affinity of both regulators for arsenite, we conducted
320 Isothermal Titration Calorimetry experiments (41). However, titrations of both
321 paralogues with arsenite, conducted at several analysis temperatures, revealed only
322 minor binding heats changes, which did not permit the calculation of binding
323 parameters. We have therefore resorted to intrinsic tryptophan fluorescence
324 spectroscopy measurements (42). The inspection of the ArsR2 homology model
325 revealed the presence of a Trp residue (W79) in immediate vicinity of cysteines 43 and
326 45 that are involved in ligand binding (Supp. Fig. 1). Following excitation at 290 nm the
327 emission spectra showed maxima at 336 nm (Fig. 5). Addition of different
328 concentrations of arsenite caused fluorescence quenching. The plot of corrected
329 fluorescence at the maximum of emission as a function of arsenite concentration is

Applied and Environmental Microbiology

shown in Fig. 5C. Data fitting resulted in K_D values of approximately 30 µM for both paralogues (Table 4).

Evidence for ArsR1 and ArsR2 cross talk

The DNA segments encoding the *ars1* and *ars2* operons are highly homologous. However, the sequences of both target promoters, P_{ars1} and P_{ars2}, show significant sequence divergence (Supp. Fig. 4). To assess whether ArsR1 and ArsR2 bind to both, or to exclusively its cognate promoter we conducted EMSA assays using purified ArsR1 and ArsR2 as well as DNA fragments covering both promoter regions. Although a wide variety of experimental conditions were tested, satisfactory EMSAs could only be obtained for promoter P_{ars1} (Fig. 6). Interestingly, both proteins bound to the P_{ars1} fragment. A single protein-DNA complex with an estimated K_D in the sub-micromolar range could be detected for ArsR2. In contrast, ArsR1 appears to form multiple DNA complexes. No binding was observed to control DNA. Unfortunately, when experiments were repeated in the presence of arsenite and arsenate, a smear and no distinct bands appeared, which made an interpretation impossible. The fact that both paralogues bind to P_{ars1} suggests the existence of cross-talk between both systems.

Construction and validation of KT2440-based arsenic biosensors

To generate whole-cell biosensors, the *arsR1* and *arsR2* sequences and their respective promoter regions were cloned into pMP220 to generate the transcriptional fusions P_{ars1}*_ars1_lacZ* and P_{ars2}*_ars2_lacZ* respectively. The resulting plasmids were inserted into *P. putida* KT2440 to give rise to biosensors Bs_WtR1 and Bs_WtR2. Beta-galactosidase measurements were made to assess biosensor function. Initial experiments were conducted to determine the influence of bacterial growth phase, temperature and

Applied and Environmental Microbiology

time of response on the performance of the different biosensors. As shown in Fig. 7A and B, cells induced in the logarithmic phase gave stronger responses than those induced in the stationary phase. Paez-Espino *et al.* reported that at 15°C products of the *ars2* operon afforded a much higher resistance to arsenite than those of *ars1* (15). To assess the influence of temperature, cultures were grown at 30 ºC to early logarithmic phase, arsenite was added and then cultures were continued at either 30 or 15 ºC. Figures 7 shows that the reduction in the temperature translated into a reduced response for both sensors. Experiments at 30 ºC showed that biosensor Bs_WtR1 gave stronger responses than the Bs_WtR2 counterpart (Fig. 7A). Responses were detected as early as 15 minutes after arsenite addition, whereas maximal readings were obtained following a 3 hour incubation. The onset of response was at approximately 10 ppb (parts per billion) and the sensitivity of biosensors is studied in further detail below. Maximal responses are obtained at a concentration of 10 000 ppb, whereas at a concentration of 100 000 ppb a very significant drop in activity was measured which is due to toxicity.

ArsB mutant based biosensors show higher sensitivity and higher magnitude of response as compared to wt based sensors

It has been shown that a mutant in the arsenic efflux pumps ArsB1 and ArsB2 (Fig. 1) is more sensitive to arsenic than the wt (14), which is due to the cellular arsenite accumulation. To verify whether this accumulation translates into higher biosensor sensitivity, two additional biosensors were constructed in which both transcriptional fusions were inserted into the ArsB1/ArsB2 double mutant to give rise to biosensors Bs_MutR1 and Bs_MutR2. The dose-response curves of all four biosensors to arsenate and arsenite are shown in Fig. 8 (A, B). We noted that mutant based biosensors caused a higher magnitude of response as compared to the biosensors using the wt strain.

Response pattern for arsenate and arsenite differed significantly. Whereas at 100 000 ppb arsenite a strong reduction in response was noted (due to toxicity), maximal responses for arsenate were observed at an analyte concentration of 100 000 ppb.

A characteristic feature of any analytical tool is their sensitivity or the lowest analyte concentration at which significant readings are obtained. To assess the sensitivity of the four biosensors, their responses in the concentration window between 1-16 ppb arsenite were determined. Analysis of data (Fig. 8C) revealed that first significant measurements were obtained at 8 ppb for the wt based sensors Bs_WtR1 and Bs_WtR2. In contrast, first statistically significant measurements were obtained at 1 or 2 ppb for both ArsB mutant based biosensors BS_MutR1 and Bs_MutR2, respectively. These data thus demonstrate that the mutation of both arsenite efflux pumps not only translated into higher magnitudes of response but also into a significant increase in biosensor sensitivity. These results differ from analogous experiments using *E. coli* where the mutation of the arsenite efflux pump did not cause an increase in biosensor sensitivity (43).

Biosensors also respond to trivalent salts of antimony

In vivo gene expression studies have shown that *E. coli* ArsR responds next to arsenate and arsenite also to trivalent salts of antimony and bismuth (24). To verify whether this is also the case for the *P. putida* paralogues, we conducted a series of gene expression studies. Data show that ArsR1 and ArsR2 mediate significant responses to antimony (Supp. Fig. 5), which were particularly pronounced for ArsR1. Interestingly, the response of wt and ArsB mutant based biosensors were similar, strongly suggesting that antimony is not an ArsB pump substrate. Responses observed for bismuth (Supp. Fig. 5) were negligible as compared to those measured for arsenate, arsenite and

antimony. To verify whether antimony and bismuth bind to the purified ArsR paralogues, we conducted fluorescence titration assays similar to those shown with arsenite in Fig. 5. Antimony bound to both paralogues with affinities comparable to those for arsenite (Table 4). Surprisingly, the tightest binding ligand was bismuth (K_D values of 9 and 6 μM for ArsR1 and ArsR2, respectively), which contrasted with the extremely weak response *in vivo*. This may be due to limitations in bismuth uptake.

Phosphate does not interfere with the performance of arsenite biosensors

A major limitation of other arsenic biosensors is the interference by inorganic phosphate (38-40). To assess any possible interference of inorganic phosphate in the functioning of the arsenite biosensors, the response of Bs-WtR1 and Bs-WtR2 to 1000 ppb arsenite in the absence and presence of up to 100 mM inorganic phosphate was monitored. As shown in Supp. Fig. 5 the presence of inorganic phosphate did not cause any significant interference with the biosensors. These data agree with the above reported absence of inorganic phosphate binding to ArsR1 and ArsR2 *in vitro* (Fig. 4).

Use of the arsenic biosensors for the analysis of environmental samples

To assess the suitability of the biosensors developed to analyze environmental samples, we carried out experiments with water recovered from a mine. This sample was submitted to an Inductively Coupled Plasma-Optical Emission Spectroscopy to precisely quantify the arsenic content. These measurements resulted in an arsenic concentration of 596 ± 32 ppb. The analysis of 1:10 diluted samples using the four different biosensors is shown in Supp. Fig. 6, demonstrating that all biosensors were able to detect arsenic. Strongest signals were obtained by the two ArsB mutant based sensors confirming the above conclusions that these sensors possess higher sensitivities.

These measurements illustrate the usefulness of the developed biosensors to detect low concentrations of arsenic in environmental samples.

Applied and Environmental Microbiology

Discussion

As mentioned in the introduction the duplication of *ars* operons appears to be a more general strategy of bacteria to enhance arsenic resistance and the double *ars* operons in *P. putida* are a model system to study the coexisting *ars* resistance systems. A number of *in vivo* studies have been published on this model (14, 15), which contrasts with the absence of any biochemical or biophysical data on these proteins.

An unusual feature of ArsR regulators is that there are at least three different modes by which arsenite is recognized. In all three cases a cysteine triad binds arsenite but the location of these residues in the structure differ for proteins of *E. coli* (27), *Corynebacterium glutamicum* (28) and *Acidithiobacillus ferrooxidans* (29) (Supp. Fig. 1). The sequence alignment shows that the *P. putida* proteins employ yet another binding mechanism, since none of the identified cysteine triads are conserved. The ArsR2 sequence motif C-X-C-$(X)_3$-C may correspond to a version of the *E. coli* binding motif of C-X-C-$(X)_2$-C. ArsR1 has a C-X-C motif, but the position of the two other cysteine residues is not conserved. We show here that despite this difference both paralogues bind arsenite with a similar affinity of around 30 µM. These similarities in affinities may at least partially account for the similarities in sensitivity of ArsR1 and ArsR2 based biosensors (Fig. 8C).

To our knowledge these are the first direct binding studies *in vitro*, although others reported arsenite binding to the regulators based on the capacity of arsenite to trigger protein release from DNA. Using such an approach an apparent K_D of 12 µM was reported for arsenite binding to ArsR of *Acidithiobacillus ferrooxidans* (29) or 150 µM for *Corynebacterium glutamicum (28)*.

E. coli ArsR, the primary model protein, shows only a modest sequence similarity between ArsR1 (40 % identity) and ArsR2 (42 % identity). However, there

458 are clear parallels in their ligand susceptibilities suggesting that these are features
459 common to the family of ArsR proteins. 1) *In vivo* experiments of *P. putida* and *E. coli*
460 ArsR show strong comparable responses to arsenite, arsenate and antimony (Figs. 8 and
461 9) (24). In both cases very minor responses were observed for bismuth. 2) *In vitro* and
462 *in vivo* data show that inorganic phosphate does not act on ArsR (Fig. 4, Supp. Fig.
463 5)(24) 3). Data show that arsenite, antimony and bismuth, but not arsenate, bind to the
464 ArsR proteins (Figs. 4, 5)(24). An unexpected finding was that bismuth, that caused
465 only weak responses *in vivo*, bound with significant affinities to ArsR1 and ArsR2
466 (Table 4). A similar discrepancy between *in vitro* binding and in *vivo* efficiency has
467 been observed for antimony binding to ArsR of *C. glutamicum* for which a K_D of 10 µM
468 was determined, a value lower than the corresponding one for arsenite (K_D=150 µM).
469 As suggested by these authors the differences may be caused by a relatively poor uptake
470 of antimony or bismuth as compared with arsenite.

471 Our demonstration that ArsR1 and ArsR2 are dimeric coincides with similar
472 findings of homologous proteins in *E. coli* and *Acidithiobacillus ferrooxidans* (29, 44),
473 suggesting that the dimeric state may also be a feature common to the ArsR protein
474 family. We have shown here that effector binding did not cause any alterations to the
475 oligomeric state of ArsR, which is an issue that has so far not been investigated.

476 The construction of a significant number of whole-cell arsenic biosensors has
477 been reported in the literature (30, 31) which hence raises the question why yet further
478 sensors were constructed. However, most of the biosensors use *E. coli* as host, whereas
479 none have been reported using *P. putida* strains. The choice of the latter organism was
480 based on its stunning resistance to a wide range of natural and anthropogenic stresses
481 like metals, organic solvents and pollutants and the ease to adapt to changing physico-
482 chemical parameters of the environment like water and oxidative stress or pH changes

Applied and Environmental Microbiology

(21, 45-48). Considering that *in situ* arsenite detection will involve the analysis of complex samples of different nature, the use of a robust bacterium is likely to confer robustness to the analysis.

The World Health Organization (WHO) has fixed the maximum level of arsenic in drinking water to 10 ppb and the Food and Agriculture Organization (FAO) has set a maximum arsenic level of 100 ppb in irrigation water (49). As shown in Fig. 8C the AsR1 and ArsR2 based biosensors can be used to assess the quality of drinking and irrigation water. Both biosensors based on the native *P. putida* strain had a sensitivity of 8 ppb. In contrast, the biosensors based on the double mutant of the arsenic afflux pumps were effective to detect 1 and 2 ppb. These data indicate that the intracellular arsenic level is higher in the double mutant than in the wt strain, which is due to the perturbation of arsenite efflux.

A biosensor based on the mutant of the *ars* operon in *E. coli* has also been reported (43). However, in contrast to our findings the elimination of the arsenic efflux pump did not translate into an improved of biosensor performance. The sensitivity of our biosensors is superior to that for the majority of whole-cell arsenic sensors reported (30).

A major hurdle for the successful construction of arsenic biosensors is the interference with inorganic phosphate (30), which has been observed in a number of cases (50-52). We show here that both ArsR paralogues do not bind inorganic phosphate (Fig. 4) and that inorganic phosphate concentrations as high as 100 mM do not interfere with arsenite sensing (Supp. Fig. 5). Another undesirable property of biosensors is their elevated background signal (43, 51, 53-55). Biosensors described here are characterized by very low background signals and a β-galactosidase activity of approximately 10 Miller Units was observed in the absence of ligand, translating into

very favorable signal to noise ratios for arsenic measurements. Measurements conducted were based on an analyte incubation time of 3 hours which is comparable to most other sensors described (30).

These analytical parameters combined with the robustness of the host strain make the biosensors constructed convenient and robust analytical tools for arsenite detection in diverse and complex samples. The enhancement of biosensor sensitivity and magnitude of response by deleting the efflux pump of the cognate analyte may be an interesting strategy for the construction of biosensors for other analytes.

Acknowledgements

The authors are grateful to Dr. Abdelali Daddaoua for valuable advice in setting up the EMSA experiments. We would like to thank the Biophysics and Molecular Biotechnology group from the Department of Physical Chemistry (University of Granada) permitting access to the DSC and CD instruments.

Funding Information

We acknowledge financial support from FEDER funds and Fondo Social Europeo through grants the Spanish Ministry for Economy and Competitiveness (RECUPERA grant 20134R057 to T.K. and grant BIO2013-42297 to T.K.) from the Junta de Andalucía (grant CVI-7335 to T.K).

529 **References**

530

531 1. **Slyemi D, Bonnefoy V.** 2012. How prokaryotes deal with arsenic(dagger).
532 Environ Microbiol Rep **4:**571-586.

533 2. **McCarty KM, Hanh HT, Kim KW.** 2011. Arsenic geochemistry and human
534 health in South East Asia. Rev Environ Health **26:**71-78.

535 3. **Argos M, Ahsan H, Graziano JH.** 2012. Arsenic and human health:
536 epidemiologic progress and public health implications. Rev Environ Health
537 **27:**191-195.

538 4. **Singh R, Singh S, Parihar P, Singh VP, Prasad SM.** 2015. Arsenic
539 contamination, consequences and remediation techniques: a review. Ecotoxicol
540 Environ Saf **112:**247-270.

541 5. **Ahmed A, Edward A, Burnham G.** 2004. Health indicators for mothers and
542 children in rural Herat Province, Afghanistan. Prehosp Disaster Med **19:**221-
543 225.

544 6. **Mukherjee A, Sengupta MK, Hossain MA, Ahamed S, Das B, Nayak B,**
545 **Lodh D, Rahman MM, Chakraborti D.** 2006. Arsenic contamination in
546 groundwater: a global perspective with emphasis on the Asian scenario. J Health
547 Popul Nutr **24:**142-163.

548 7. **Merulla D, Buffi N, Beggah S, Truffer F, Geiser M, Renaud P, van der**
549 **Meer JR.** 2013. Bioreporters and biosensors for arsenic detection.
550 Biotechnological solutions for a world-wide pollution problem. Curr Opin
551 Biotechnol **24:**534-541.

552 8. **Ron EZ.** 2007. Biosensing environmental pollution. Curr Opin Biotechnol
553 **18:**252-256.

554 9. **Dopson M, Baker-Austin C, Koppineedi PR, Bond PL.** 2003. Growth in
555 sulfidic mineral environments: metal resistance mechanisms in acidophilic
556 micro-organisms. Microbiology **149:**1959-1970.
557 10. **Baker-Austin C, Dopson M, Wexler M, Sawers RG, Stemmler A, Rosen BP,**
558 **Bond PL.** 2007. Extreme arsenic resistance by the acidophilic archaeon
559 '*Ferroplasma acidarmanus*' Fer1. Extremophiles **11:**425-434.
560 11. **San Francisco MJ, Hope CL, Owolabi JB, Tisa LS, Rosen BP.** 1990.
561 Identification of the metalloregulatory element of the plasmid-encoded arsenical
562 resistance operon. Nucleic Acids Res **18:**619-624.
563 12. **Paez-Espino D, Tamames J, de Lorenzo V, Canovas D.** 2009. Microbial
564 responses to environmental arsenic. BioMetals **22:**117-130.
565 13. **Nelson KE, Weinel C, Paulsen IT, Dodson RJ, Hilbert H, Martins dos**
566 **Santos VA, Fouts DE, Gill SR, Pop M, Holmes M, Brinkac L, Beanan M,**
567 **DeBoy RT, Daugherty S, Kolonay J, Madupu R, Nelson W, White O,**
568 **Peterson J, Khouri H, Hance I, Chris Lee P, Holtzapple E, Scanlan D, Tran**
569 **K, Moazzez A, Utterback T, Rizzo M, Lee K, Kosack D, Moestl D, Wedler**
570 **H, Lauber J, Stjepandic D, Hoheisel J, Straetz M, Heim S, Kiewitz C, Eisen**
571 **JA, Timmis KN, Dusterhoft A, Tummler B, Fraser CM.** 2002. Complete
572 genome sequence and comparative analysis of the metabolically versatile
573 *Pseudomonas putida* KT2440. Environ Microbiol **4:**799-808.
574 14. **Fernandez M, Udaondo Z, Niqui JL, Duque E, Ramos JL.** 2014. Synergic
575 role of the two ars operons in arsenic tolerance in *Pseudomonas putida* KT2440.
576 Environ Microbiol Rep **6:**483-489.

15. **Paez-Espino AD, Durante-Rodriguez G, de Lorenzo V.** 2015. Functional coexistence of twin arsenic resistance systems in *Pseudomonas putida* KT2440. Environ Microbiol **17:**229-238.

16. **Ordonez E, Letek M, Valbuena N, Gil JA, Mateos LM.** 2005. Analysis of genes involved in arsenic resistance in *Corynebacterium glutamicum* ATCC 13032. Appl Environ Microbiol **71:**6206-6215.

17. **Branco R, Chung AP, Morais PV.** 2008. Sequencing and expression of two arsenic resistance operons with different functions in the highly arsenic-resistant strain *Ochrobactrum tritici* SCII24T. BMC Microbiol **8:**95.

18. **Regenhardt D, Heuer H, Heim S, Fernandez DU, Strompl C, Moore ER, Timmis KN.** 2002. Pedigree and taxonomic credentials of *Pseudomonas putida* strain KT2440. Environ Microbiol **4:**912-915.

19. **Espinosa-Urgel M, Kolter R, Ramos JL.** 2002. Root colonization by *Pseudomonas putida*: love at first sight. Microbiology **148:**341-343.

20. **Jimenez JI, Canales A, Jimenez-Barbero J, Ginalski K, Rychlewski L, Garcia JL, Diaz E.** 2008. Deciphering the genetic determinants for aerobic nicotinic acid degradation: the nic cluster from *Pseudomonas putida* KT2440. Proc Natl Acad Sci U S A **105:**11329-11334.

21. **Canovas D, Cases I, de Lorenzo V.** 2003. Heavy metal tolerance and metal homeostasis in *Pseudomonas putida* as revealed by complete genome analysis. Environ Microbiol **5:**1242-1256.

22. **Chen J, Bhattacharjee H, Rosen BP.** 2015. ArsH is an organoarsenical oxidase that confers resistance to trivalent forms of the herbicide monosodium methylarsenate and the poultry growth promoter roxarsone. Mol Microbiol **96:**1042-1052.

23. **Osman D, Cavet JS.** 2010. Bacterial metal-sensing proteins exemplified by ArsR-SmtB family repressors. Nat Prod Rep **27:**668-680.

24. **Wu J, Rosen BP.** 1993. Metalloregulated expression of the *ars* operon. J Biol Chem **268:**52-58.

25. **Oden KL, Gladysheva TB, Rosen BP.** 1994. Arsenate reduction mediated by the plasmid-encoded ArsC protein is coupled to glutathione. Mol Microbiol **12:**301-306.

26. **Busenlehner LS, Pennella MA, Giedroc DP.** 2003. The SmtB/ArsR family of metalloregulatory transcriptional repressors: Structural insights into prokaryotic metal resistance. FEMS Microbiol Rev **27:**131-143.

27. **Shi W, Wu J, Rosen BP.** 1994. Identification of a putative metal binding site in a new family of metalloregulatory proteins. J Biol Chem **269:**19826-19829.

28. **Ordonez E, Thiyagarajan S, Cook JD, Stemmler TL, Gil JA, Mateos LM, Rosen BP.** 2008. Evolution of metal(loid) binding sites in transcriptional regulators. J Biol Chem **283:**25706-25714.

29. **Qin J, Fu HL, Ye J, Bencze KZ, Stemmler TL, Rawlings DE, Rosen BP.** 2007. Convergent evolution of a new arsenic binding site in the ArsR/SmtB family of metalloregulators. J Biol Chem **282:**34346-34355.

30. **Kaur H, Kumar R, Babu JN, Mittal S.** 2015. Advances in arsenic biosensor development--a comprehensive review. Biosens Bioelectron **63:**533-545.

31. **Merulla D, Buffi N, Beggah S, Truffer F, Geiser M, Renaud P, van der Meer JR.** 2013. Bioreporters and biosensors for arsenic detection. Biotechnological solutions for a world-wide pollution problem. Curr Opin Biotechnol **24:**534-541.

626 32. **Gasteiger E, C. H, A. G, S. D, M.R. W, R.D. A, A. B.** 2005. Protein
627 Identification and Analysis Tools on the ExPASy Server. (In) John M. Walker
628 (ed): The Proteomics Protocols Handbook, Humana Press (2005)**:**571-607.
629 33. **Bohm G, Muhr R, Jaenicke R.** 1992. Quantitative analysis of protein far UV
630 circular dichroism spectra by neural networks. Protein Eng **5:**191-195.
631 34. **van de Weert M.** 2010. Fluorescence quenching to study protein-ligand
632 binding: common errors. J Fluoresc **20:**625-629.
633 35. **Miller JE.** 1972. Experiments in Molecular Genetics. Cold Spring Harbor
634 Laboratory, Cold Spring Harbor, New York**:**466 pp.
635 36. **Xu C, Shi W, Rosen BP.** 1996. The chromosomal arsR gene of *Escherichia coli*
636 encodes a *trans*-acting metalloregulatory protein. J Biol Chem **271:**2427-2432.
637 37. **Chiu MH, Prenner EJ.** 2011. Differential scanning calorimetry: An invaluable
638 tool for a detailed thermodynamic characterization of macromolecules and their
639 interactions. J Pharm Bioallied Sci **3:**39-59.
640 38. **Hughes MF.** 2002. Arsenic toxicity and potential mechanisms of action.
641 Toxicol Lett **133:**1-16.
642 39. **Gonzalez D, Richez M, Bergonzi C, Chabriere E, Elias M.** 2014. Crystal
643 structure of the phosphate-binding protein (PBP-1) of an ABC-type phosphate
644 transporter from *Clostridium perfringens*. Sci Rep **4:**6636.
645 40. **Beene LC, Halluer J, Yoshinaga M, Hamdi M, Liu Z.** 2011. Pentavalent
646 arsenate transport by zebrafish phosphate transporter NaPi-IIb1. Zebrafish
647 **8:**125-131.
648 41. **Krell T.** 2008. Microcalorimetry: a response to challenges in modern
649 biotechnology. Microb Biotechnol **1:**126-136.

42. **Eftink MR.** 1997. Fluorescence methods for studying equilibrium macromolecule-ligand interactions. Methods Enzymol **278:**221-257.

43. **Tauriainen S, Virta M, Chang W, Karp M.** 1999. Measurement of firefly luciferase reporter gene activity from cells and lysates using *Escherichia coli* arsenite and mercury sensors. Anal Biochem **272:**191-198.

44. **Xu C, Rosen BP.** 1997. Dimerization is essential for DNA binding and repression by the ArsR metalloregulatory protein of *Escherichia coli*. J Biol Chem **272:**15734-15738.

45. **Nikel PI, de Lorenzo V.** 2014. Robustness of *Pseudomonas putida* KT2440 as a host for ethanol biosynthesis. N Biotechnol **31:**562-571.

46. **Dominguez-Cuevas P, Gonzalez-Pastor JE, Marques S, Ramos JL, de Lorenzo V.** 2006. Transcriptional tradeoff between metabolic and stress-response programs in *Pseudomonas putida* KT2440 cells exposed to toluene. J Biol Chem **281:**11981-11991.

47. **Chavarria M, Nikel PI, Perez-Pantoja D, de Lorenzo V.** 2013. The Entner-Doudoroff pathway empowers *Pseudomonas putida* KT2440 with a high tolerance to oxidative stress. Environ Microbiol **15:**1772-1785.

48. **Timmis KN.** 2002. *Pseudomonas putida*: a cosmopolitan opportunist par excellence. Environ Microbiol **4:**779-781.

49. **Rahaman S, Sinha AC, Pati R, Mukhopadhyay D.** 2013. Arsenic contamination: a potential hazard to the affected areas of West Bengal, India. Environ Geochem Health **35:**119-132.

50. **Cai J, DuBow MS.** 1997. Use of a luminescent bacterial biosensor for biomonitoring and characterization of arsenic toxicity of chromated copper arsenate (CCA). Biodegradation **8:**105-111.

675 51. **Liao VH, Ou KL.** 2005. Development and testing of a green fluorescent
676 protein-based bacterial biosensor for measuring bioavailable arsenic in
677 contaminated groundwater samples. Environ Toxicol Chem **24:**1624-1631.
678 52. **Ivanina AV, Shuvaeva OV.** 2009. Use of a bacterial biosensor system for
679 determining arsenic in natural waters. J Anal Chem **64**.
680 53. **Scott DL, Ramanathan S, Shi W, Rosen BP, Daunert S.** 1997. Genetically
681 engineered bacteria: electrochemical sensing systems for antimonite and
682 arsenite. Anal Chem **69:**16-20.
683 54. **Roberto FF, Barnes JM, Bruhn DF.** 2002. Evaluation of a GFP reporter gene
684 construct for environmental arsenic detection. Talanta **58:**181-188.
685 55. **Tani C, Inoue K, Tani Y, Harun-ur-Rashid M, Azuma N, Ueda S, Yoshida**
686 **K, Maeda I.** 2009. Sensitive fluorescent microplate bioassay using recombinant
687 *Escherichia coli* with multiple promoter-reporter units in tandem for detection of
688 arsenic. J Biosci Bioeng **108:**414-420.
689 56. **Frazer KA, Pachter L, Poliakov A, Rubin EM, Dubchak I.** 2004. VISTA:
690 computational tools for comparative genomics. Nucleic Acids Res **32:**W273-
691 279.
692 57. **Bagdasarian M, Lurz R, Ruckert B, Franklin FC, Bagdasarian MM, Frey**
693 **J, Timmis KN.** 1981. Specific-purpose plasmid cloning vectors. II. Broad host
694 range, high copy number, RSF1010-derived vectors, and a host-vector system
695 for gene cloning in Pseudomonas. Gene **16:**237-247.
696 58. **Woodcock DM, Crowther PJ, Doherty J, Jefferson S, DeCruz E, Noyer-**
697 **Weidner M, Smith SS, Michael MZ, Graham MW.** 1989. Quantitative
698 evaluation of *Escherichia coli* host strains for tolerance to cytosine methylation
699 in plasmid and phage recombinants. Nucleic Acids Res **17:**3469-3478.

59. **Jeong H, Barbe V, Lee CH, Vallenet D, Yu DS, Choi SH, Couloux A, Lee SW, Yoon SH, Cattolico L, Hur CG, Park HS, Segurens B, Kim SC, Oh TK, Lenski RE, Studier FW, Daegelen P, Kim JF.** 2009. Genome sequences of *Escherichia coli* B strains REL606 and BL21(DE3). J Mol Biol **394:**644-652.

60. **Spaink HP, Okker RJ, Wijffelman CA, Pees E, Lugtenberg BJ.** 1987. Promoters in the nodulation region of the *Rhizobium leguminosarum* Sym plasmid pRL1JI. Plant Mol Biol **9:**27-39.

Figure legends

Fig. 1) The two paralogous *ars* operons in *P. putida* KT2440. A) Genetic organization. The transcriptional regulators ArsR are shown in red, *arsB* encodes an arsenite efflux pump, *arsH* an organoarsenical oxidase and *arsC* an arsenate reductase. Numbers below the arrows represent the intergenic distance between contiguous genes, with negative numbers indicating overlapping genes. B) DNA sequence homology between both operons. The alignments were performed using the wgVISTA (56) algorithm.

Fig. 2) Comparison of the secondary structures and thermal stabilities of the ArsR paralogues. A) Analysis of ArsR1 and ArsR2 by far UV circular dichroism spectroscopy. B) Analysis of the thermal unfolding by differential scanning calorimetry. Cp: heat capacity.

Fig. 3) Determination of the oligomeric state of both ArsR paralogues. Size exclusion chromatography of ArsR1 (A) and ArsR2 (B) in the absence (black line) and presence of 1 mM arsenite (grey line) or 1 arsenate (dashed grey line). The grey lines in the inserts show the experimentally determined v_e/v_o ratios as well as the corresponding extrapolation of the molecular weight. v_o: void volume, v_e: elution volume.

Fig. 4) Stability studies of both ArsR paralogues. Differential scanning calorimetry experiments of ArsR1 (A) and ArsR2 (B) in the absence and presence of arsenite, arsenate and inorganic phosphate. Ligands were added at a concentration of 200 µM and

the protein was at 20 µM. Derived thermodynamic parameters are given in Table 3. For clarity reasons traces were moved arbitrarily on the y-axis.

Fig. 5) Binding studies of arsenite to ArsR1 and ArsR2. Intrinsic tryptophan fluorescence spectra of 5 µM ArsR1 (A) and ArsR2 (B) in the absence (black line) and presence (colored lines) of increasing concentration of arsenite (up to 230 µM). C) Decrease in the maximum fluorescence intensity as a function of arsenite concentration. Red: ArsR1, purple: ArsR2.

Fig. 6) Binding of ArsR1 and ArsR2 to promoter P_{ars1}. Electrophoretic mobility shift assays of both ArsR paralogues using a 476 bp DNA fragment spanning the P_{ars1} promoter. The control is a DNA fragment amplified from the genome of *Serratia plymuthica*. The corresponding primers for the amplification of DNA probes are given in Table 2.

Fig. 7) Assessment of the influence of growth phase, growth temperature and time of arsenite exposure on biosensor performance. Cells were pre-grown at 30ºC and arsenite was either added to cells in the logarithmic phase (OD_{660}≈ 0.3-0.4, A and C) or stationary phase (overnight cultures). Cultures were then incubated either at 30 ºC (A and B) or 15 ºC (C). In all cases measurements were made 15, 60, 120 or 180 min after arsenite addition. Shown are means and standard deviations from three independent experiments.

Fig. 8) Biosensor response to different arsenite and arsenate concentrations. Cells were grown at 30ºC until OD_{660}=0.3-0.4 prior to the addition of either arsenite or

757 arsenate. Measurements were made three hours after induction. A, B) Dose-response
758 curves for arsenite and arsenate. C) Determination of the onset of response. Shown are
759 means and standard deviations from three independent experiments. T-students test P-
760 values: *<0.05, **<0.01 (with respect to arsenite free samples).
761

762 **Table 1) Strains and plasmids used in this study.**

Strains	**Characteristics**	**Reference**
Pseudomonas putida KT2440	Considered wild type in this study; spontaneous restriction-deficient derivative of strain mt-2 cured of the TOL plasmid pWW0	(57)
P. putida KT2440 *arsB1*/*arsB2*	Double mutant in *arsB1*/*arsB2* pCHESI::*ars1*/ miniTn*5*::*ars2* (Km^R; Gm^R)	(14)
Escherichia coli DH5α	*supE44 lacU169*(*Ø80lacZΔ M15*) *hsdR17* ($r_K^- m_K^-$) *recA1 endA1 gyrA96 thi-1 relA1*	(58)
E. coli BL21(DE3)	F–, *ompI, hsdS*$_B$ (r_B^- m_B^-) *gal*, *dam*, *met*	(59)

Plasmids		
pET28a	protein expression vector; Km^R	Novagen
pET_arsR1	pET28a containing *arsR1*; Km^R	This work
pET_arsR2	pET28a containing *arsR2*; Km^R	This work
pMP220	Transcriptional fusion vector; *lacZ*; Tc^R	(60)
pBiosen_arsR1	Transcriptional fusion P_{ars1}_*ars1*_*lacZ* in pMP220; Tc^R	This work
pBiosen_arsR2	Transcriptional fusion P_{ars2}_*ars2*_*lacZ* in pMP220; Tc^R	This work

Biosensors		
Bs_WtR1	*P. putida* KT2440 harboring pBiosen_arsR1	This work
Bs_WtR2	*P. putida* KT2440 harboring pBiosen_arsR2	This work
Bs_MutR1	*P. putida* KT2440 *arsB1*/*arsB2* harboring pBiosen_arsR1	This work
Bs_MutR2	*P. putida* KT2440 *arsB1*/*arsB2* harboring pBiosen_arsR2	This work

763 Antibiotics: Km: kanamycin; Gm: gentamycin; Tc: tetracyclin

764

765 **Table 2) Oligonucleotides used on this study**. Restriction sites are underlined.
766

Oligonucleotide	Sequence (5'-3')
Protein expression	
arsR1His_for	AACATATGATGCGAGAAATACTGACTCC (NdeI)
arsR1His_rev	TTCTCGAGTCAAGCACAAGCAACAGGGCTC (XhoI)
arsR2His_for	AACATATGATGATCACACCGCCCGATGT (NdeI)
arsR2His_rev	TTCTCGAGTCAGCAGCAGACGGAATCAC (XhoI)
Biosensor construction	
ars1biosen_for	AAGAATTCGACCGCTTCCTTCAATGCCCCC (EcoRI)
ars1biosen_rev	AACTGCAGGCGAAGGGAAGTCTCAAGCACA (PstI)
ars2biosen_for	AAGAATTCGCGTAGCCGGTGACACCGATCG (EcoRI)
ars2biosen_rev	AATCTAGAGGTGATGATCAGCAGCAGACGG (XbaI)
EMSA	
Pars1_for	GACCCTTGCGGCGATCCATCA
Pars1_rev	AAGGTCTTGGGTCGGCAAGCC
Pars2_for	TGGCGACTGATCTTGGGTTGGC
Pars2_rev	GGAGACACCTTCAGCGTAGCCG
Primers for non – specific fragments	AGAGGTAGCTCACATGAT* CATGCCGCTTCCTTGGTTT*

767 .
768 *From *Serratia plymuthica*, strain A153.
769

770 **Table 3) Thermodynamic parameters of protein unfolding monitored by DSC in**
771 **the absence and presence of different ligands.** The corresponding data are shown in
772 Fig. 4.
773

	ArsR1		ArsR2	
	T_m (ºC)[a]	ΔH_m (kJ.mol^{-1})	T_m (ºC)[a]	ΔH_m (kJ.mol^{-1})
Ligand-free	61.5	280 ± 2	71.1	265 ± 10
0.2 mM arsenite	67.5/73.4[b]	239 ± 10[c]	77.8/87.4[b]	274 ± 6[c]
0.2 mM arsenate	61.2	282 ± 9	71.5	266 ± 6
1.0 mM inorganic phosphate	61.6	277 ± 13	71.0	251 ± 5

774

775 [a] Internal calibration of the DSC equipment gives an error of +/- 0.10ºC in Tm.

776 [b] Protein unfolded in two events and both Tm values are provided

777 [c] Provided is the sum of both events

778

779 **Table 4) Interaction of different metal salts with ArsR1 and ArsR2**. Shown are
780 dissociation constants derived from fluorescence titrations of protein with different
781 ligands (See materials section for further information). Data are means and standard
782 deviations from three independent experiments.
783

	K_D (µM)	
ligand	**ArsR1**	**ArsR2**
arsenate	No binding	No binding
arsenite	30.8 ± 3	29.7 ± 1
antimony	28.1 ± 1	21.8 ± 2
bismuth	9.2 ± 1	6.3 ± 1

784

Fig. 1

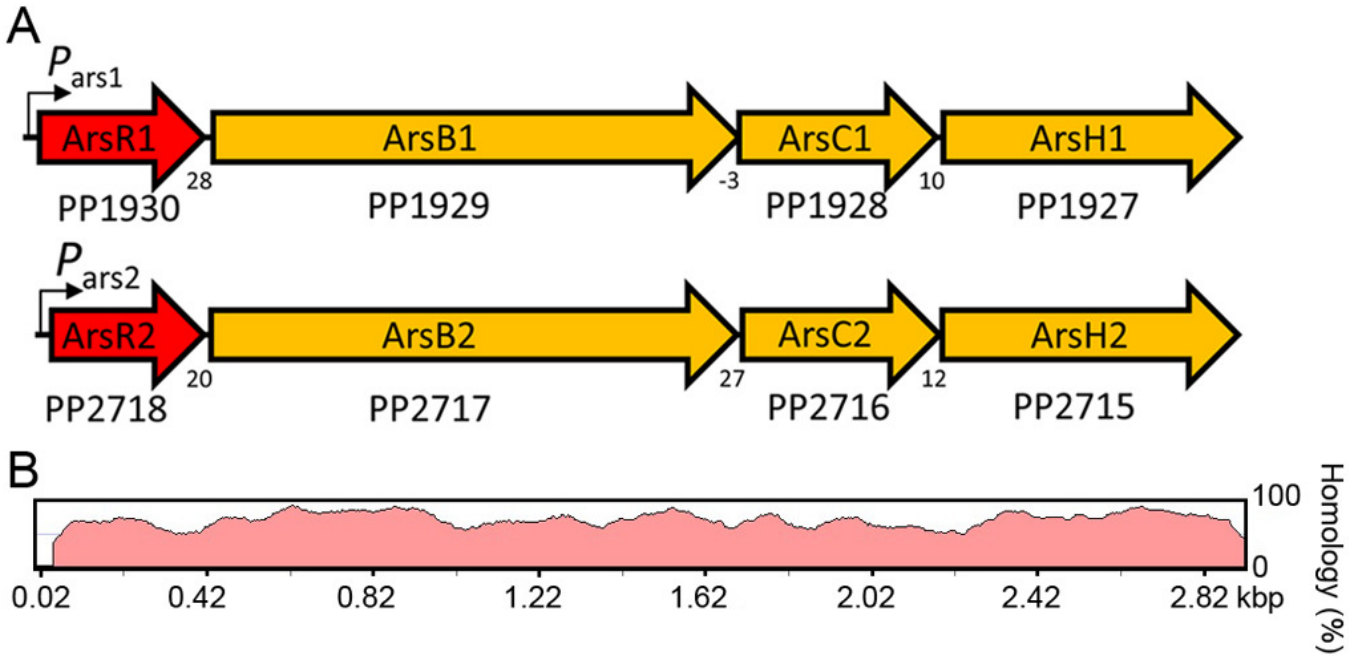

Fig. 2

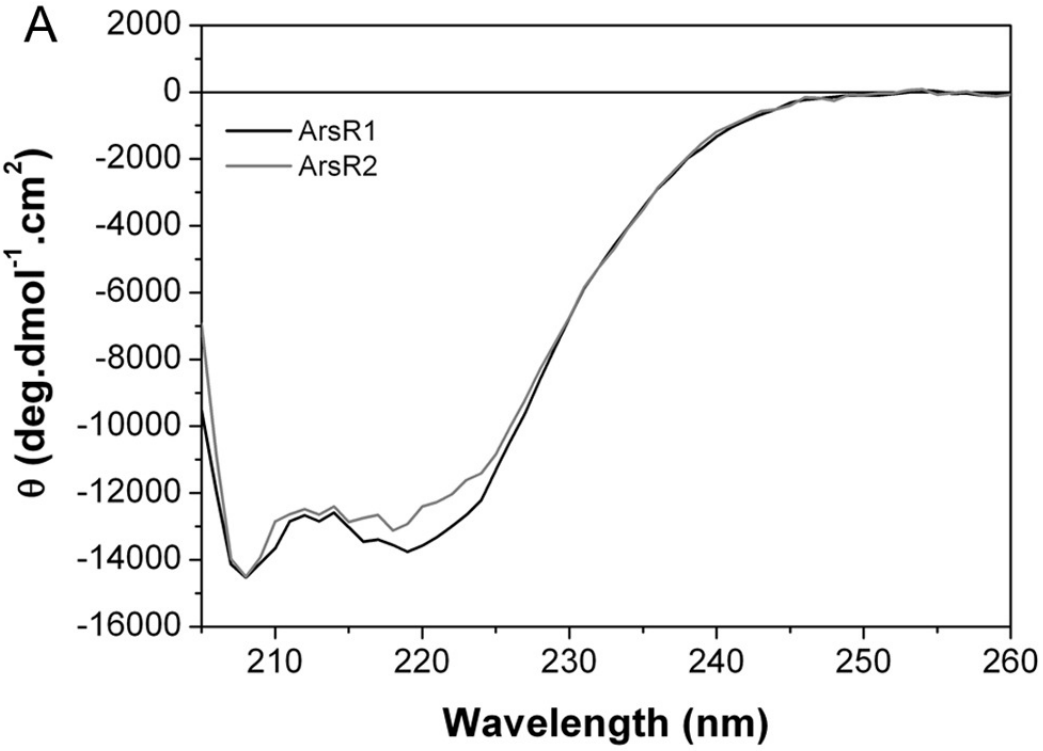

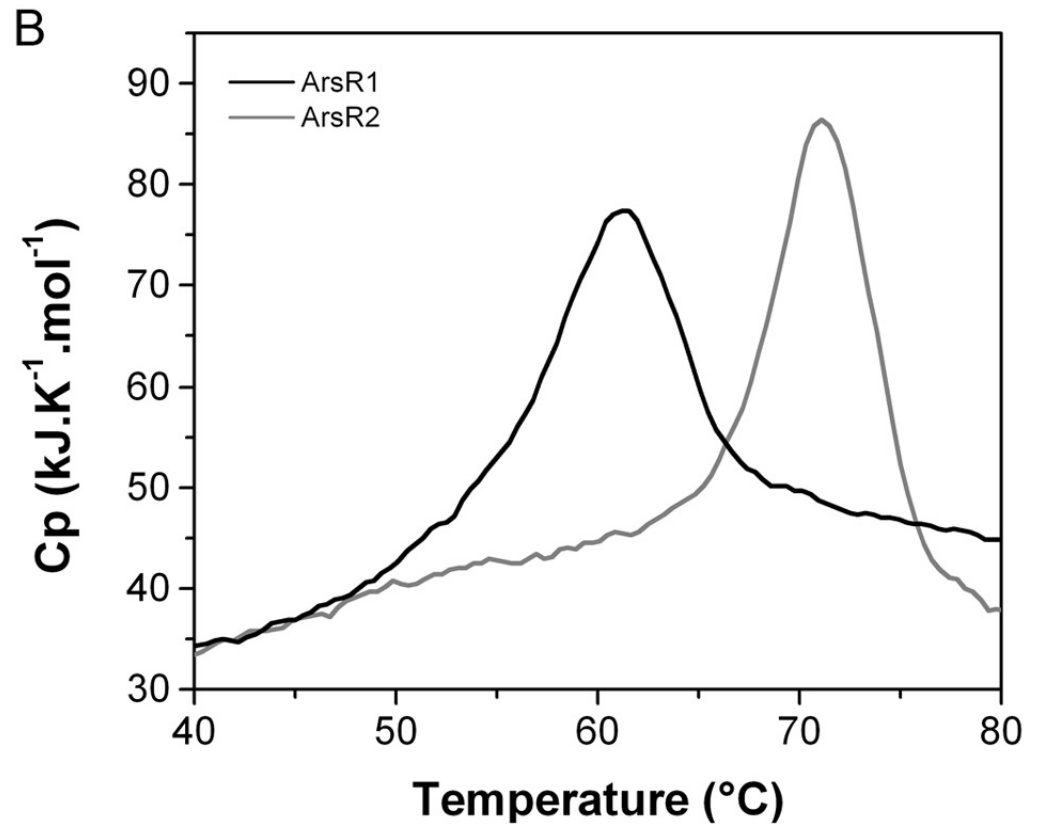

Fig. 3

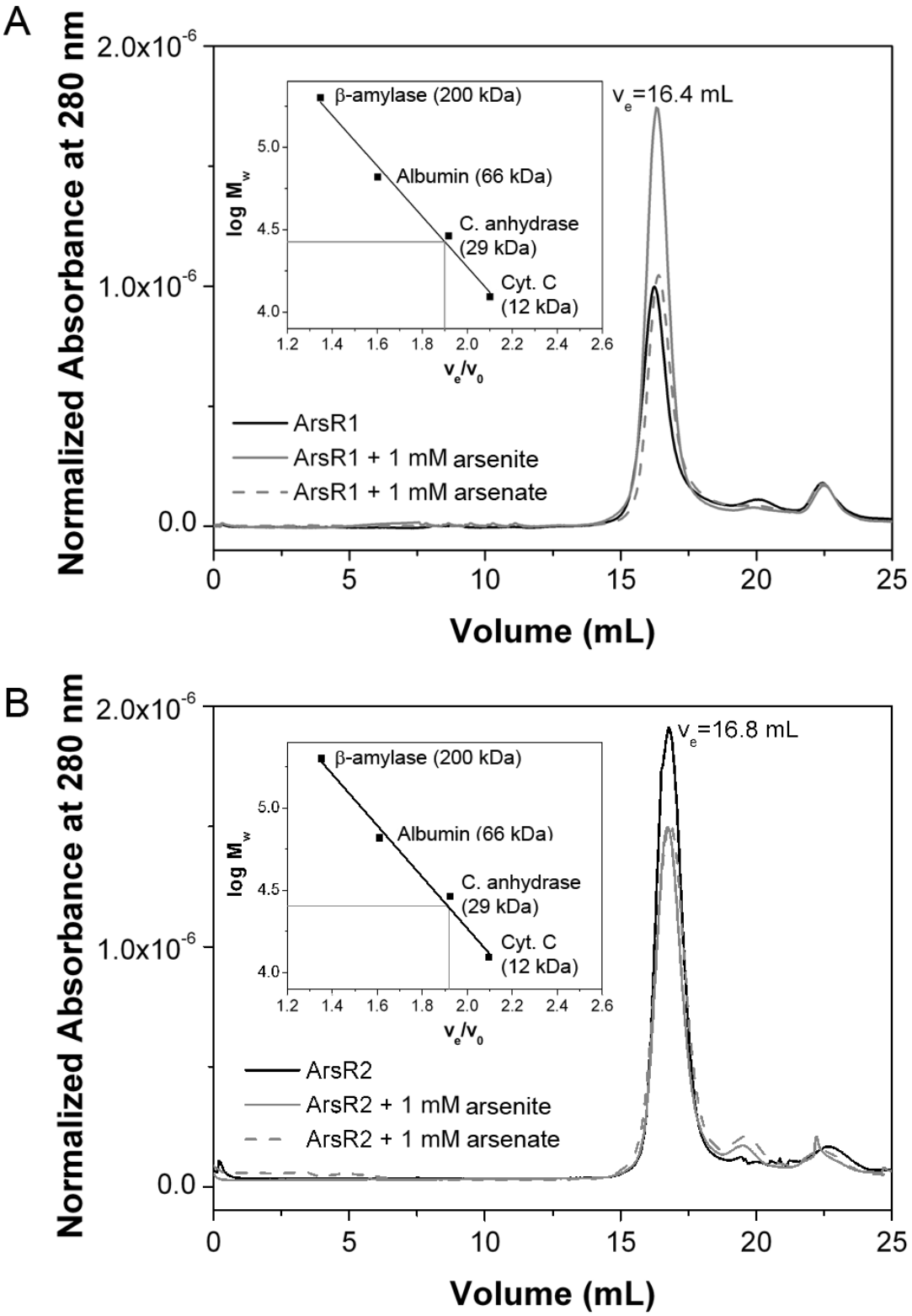

Fig. 4

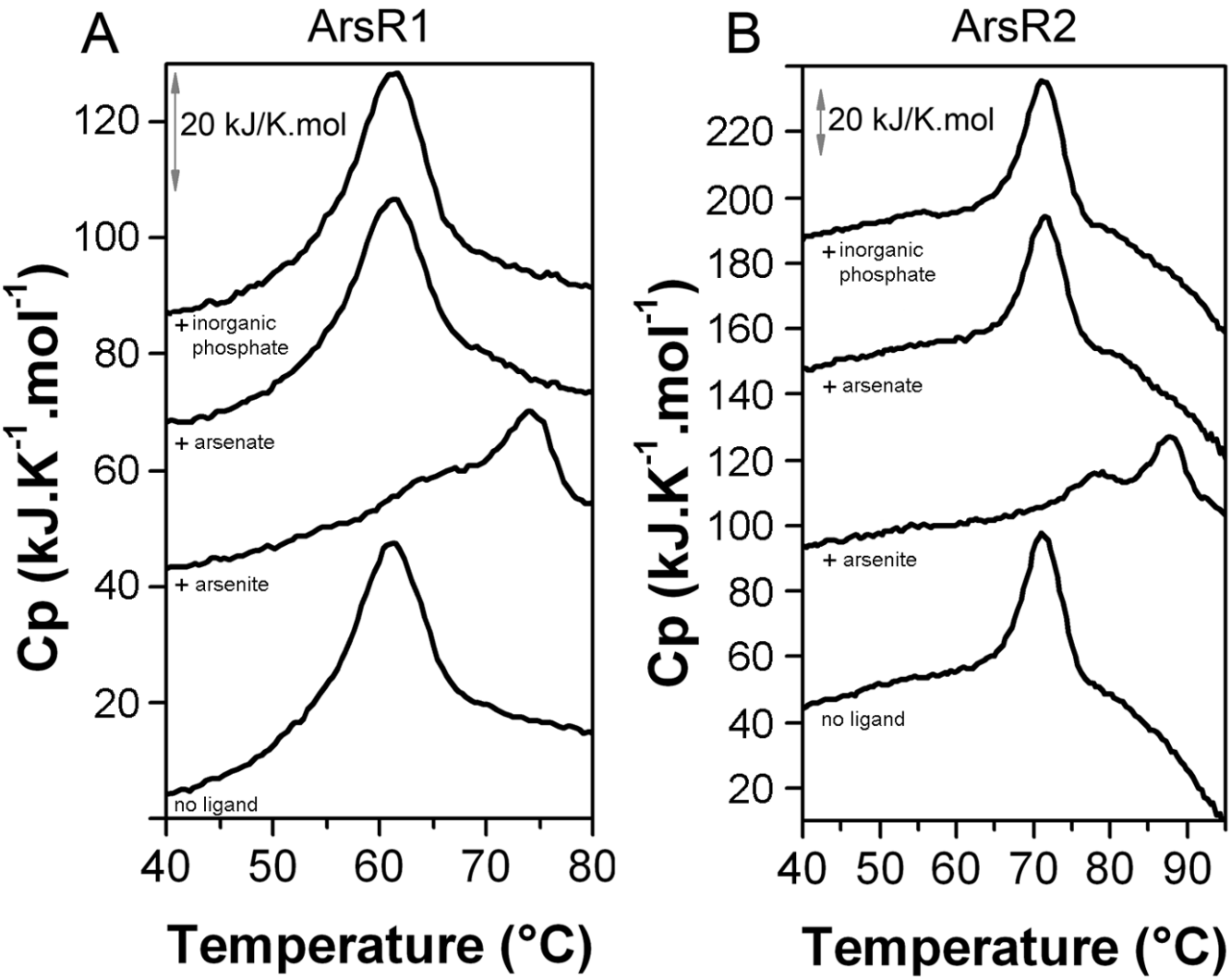

Fig. 5

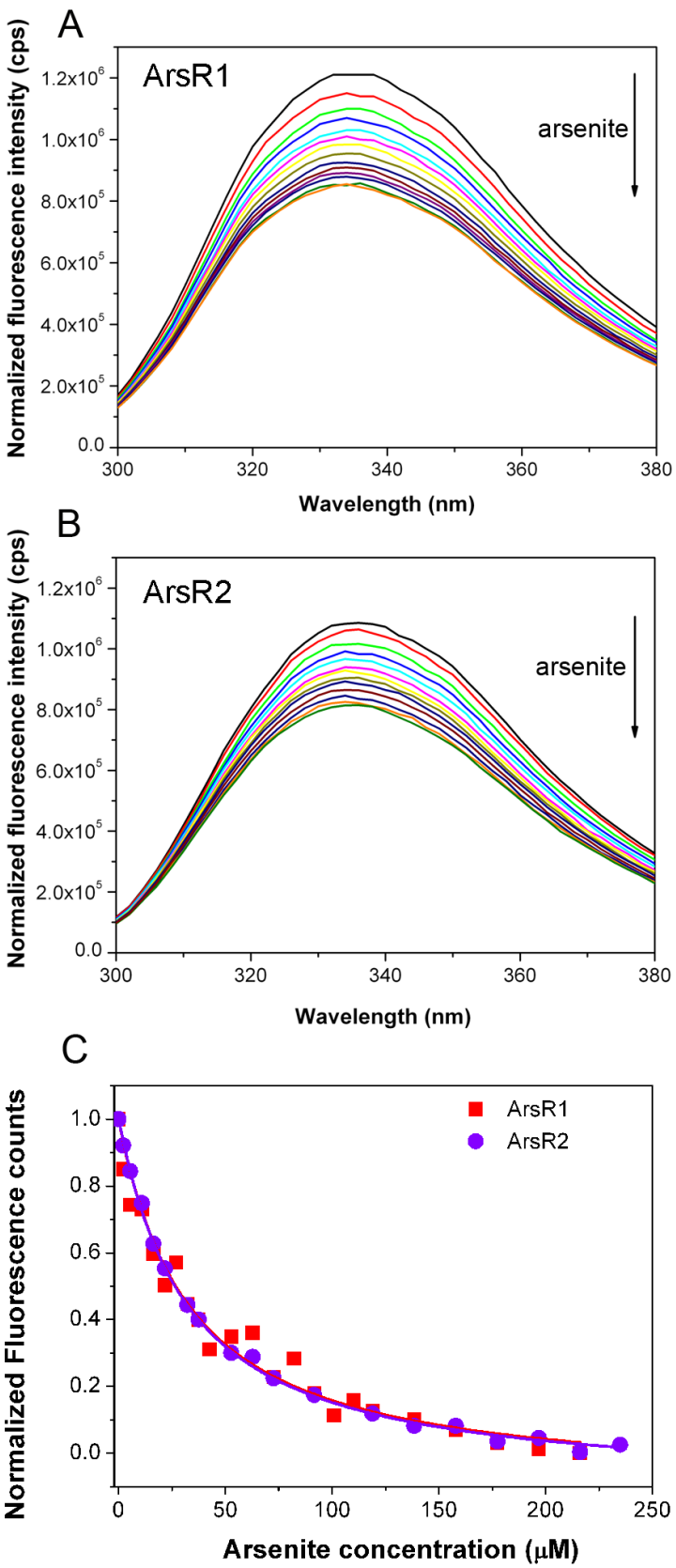

Fig. 6

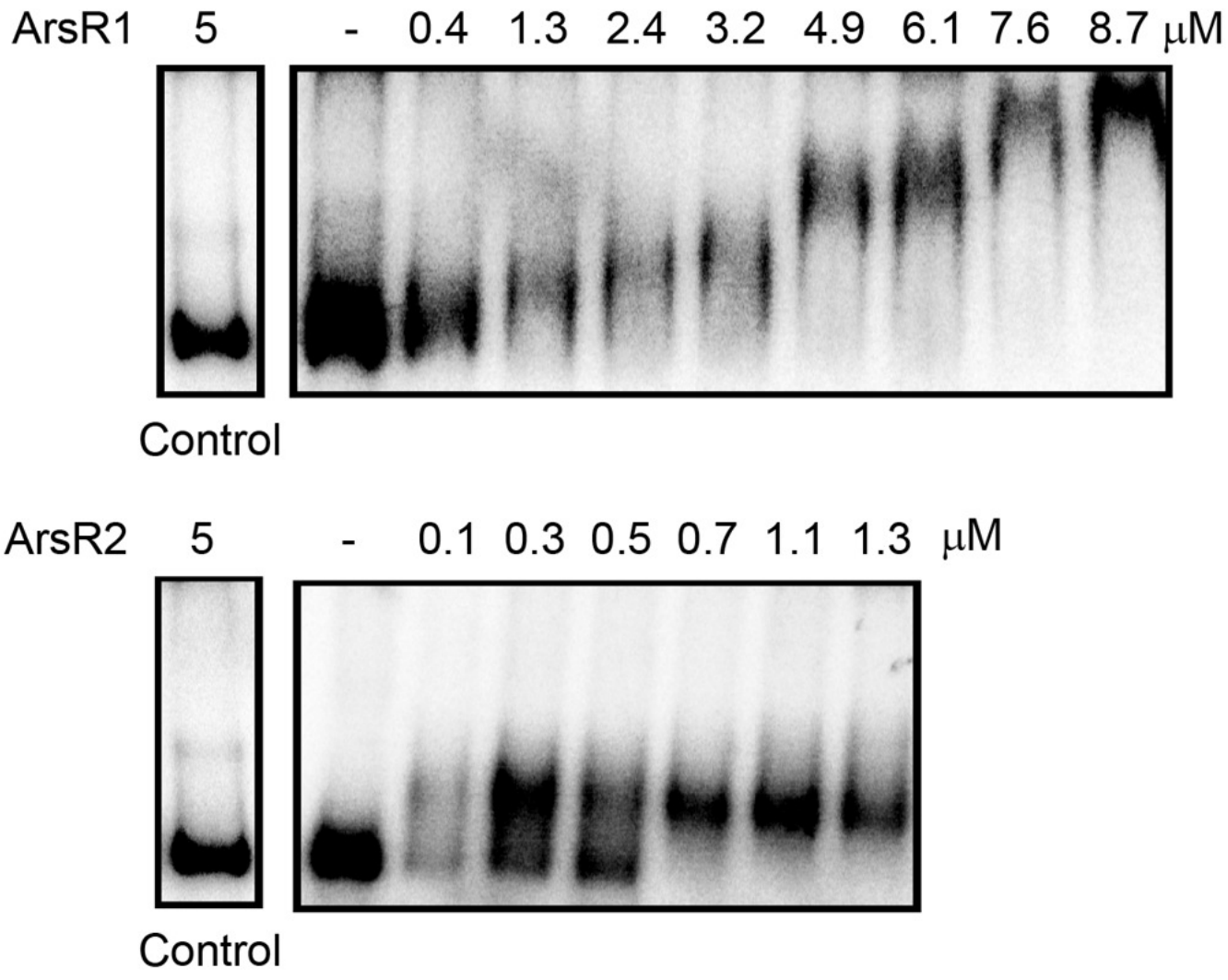

Fig. 7

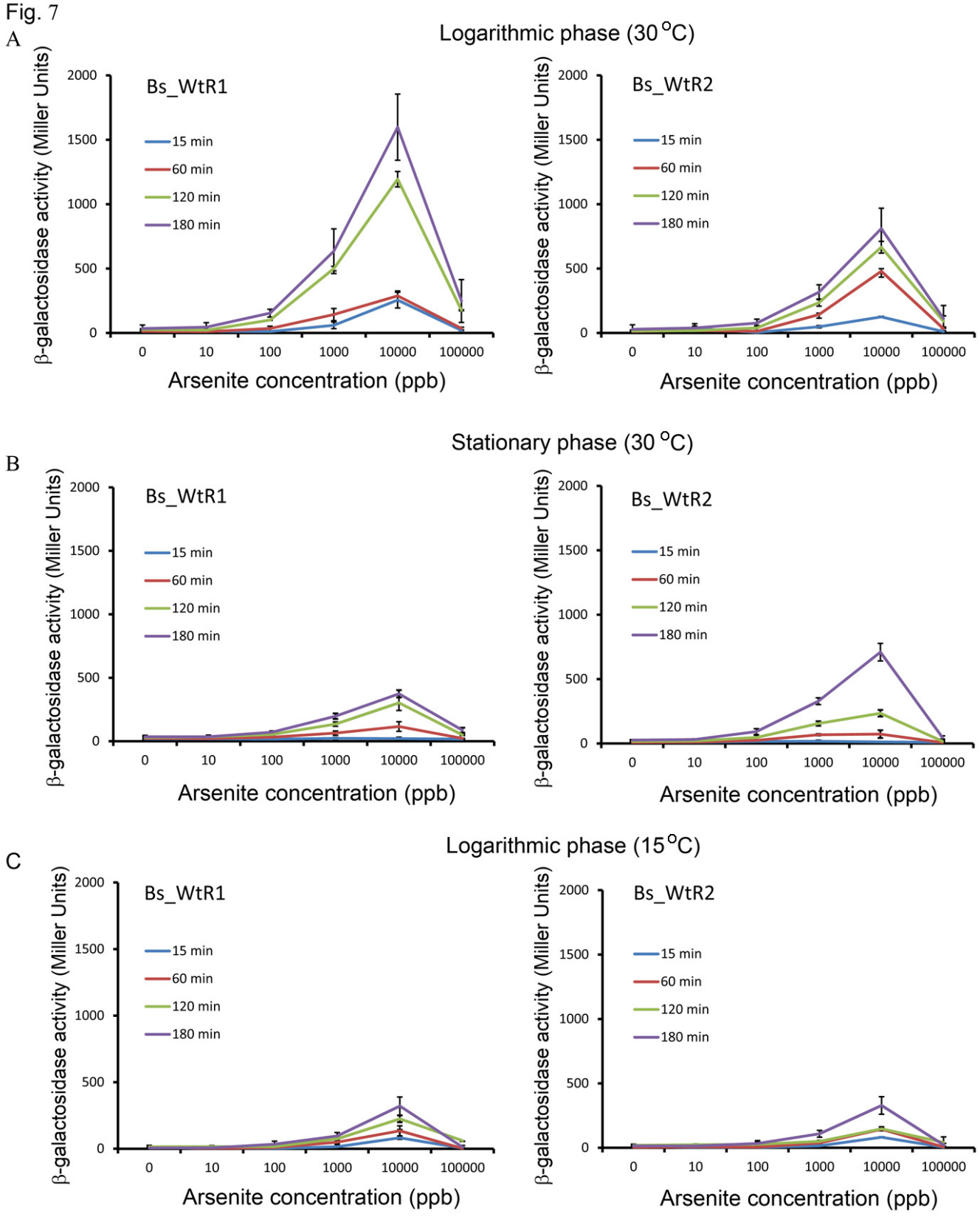

Fig. 8